Mirror system of the RICH detector of the NA62 experiment

Published by IOP Publishing for Sissa Medialab

Received: *November 3, 2017*
Accepted: *November 30, 2017*
Published: *December 12, 2017*

Mirror system of the RICH detector of the NA62 experiment

D. Aisa,[a,b] **G. Anzivino,**[a,b] **M. Barbanera,**[a,b] **M. Bizzarri,**[a,b] **A. Bizzeti,**[e,d] **F. Bucci,**[d] **C. Campeggi,**[a,b] **V. Carassiti,**[f] **A. Cassese,**[c,d] **P. Cenci,**[b] **R. Ciaranfi,**[d] **C. David,**[g] **V. Duk,**[b] **E. Iacopini,**[c,d] **E. Imbergamo,**[a,b] **G. Latino,**[c,d] **M. Lenti,**[c,d,1] **R. Lollini,**[a,b] **F. Maletta,**[d] **M. Pepe,**[b] **M. Piccini,**[b] **A. Piluso,**[a,b] **T. Schneider,**[g] **G. Scolieri,**[b] **M. Van Stenis**[g] **and R. Volpe**[c,d]

[a] *Dipartimento di Fisica e Geologia dell'Università di Perugia, I-06123 Perugia, Italy*
[b] *INFN — Sezione di Perugia, I-06123 Perugia, Italy*
[c] *Dipartimento di Fisica e Astronomia dell'Università di Firenze, I-50019 Sesto Fiorentino, Italy*
[d] *INFN — Sezione di Firenze, I-50019 Sesto Fiorentino, Italy*
[e] *Dipartimento di Scienze Fisiche, Informatiche e Matematiche dell'Università di Modena e Reggio Emilia, I-41125 Modena, Italy*
[f] *INFN — Sezione di Ferrara, I-44122 Ferrara, Italy*
[g] *CERN, European Organization for Nuclear Research, Geneva, Switzerland*

E-mail: massimo.lenti@fi.infn.it

Abstract: A large RICH detector is used in NA62 to suppress the muon contamination in the charged pion selection by a factor 100 in the momentum range between 15 and 35 GeV/c. The detector consists of a 17 m long tank (vessel), filled with neon gas at atmospheric pressure. Cherenkov light is reflected by a mosaic of 20 spherical mirrors with 17 m focal length, placed at the downstream end, and collected by 1952 photomultipliers (PMTs) placed at the upstream end. In this paper the characterization of the mirrors before installation and the mirror support system are described. The mirror installation procedure and the laser alignment are also illustrated.

Keywords: Cherenkov detectors; Large detector systems for particle and astroparticle physics; Particle identification methods

[1] Corresponding author.

https://doi.org/10.1088/1748-0221/12/12/P12017

2017 JINST 12 P12017

Contents

2017 JINST 12 P12017

1 NA62 experiment

NA62 [1] is a fixed target experiment located in the North Area of CERN and dedicated to study charged kaon decays, in particular the very rare decay $K^+ \to \pi^+ \nu\bar{\nu}$. A 400 GeV/c momentum proton beam extracted from the CERN Super Proton Synchrotron (SPS), impinging on a beryllium target, is used to produce a secondary hadron beam. A 100 m long beam line equipped with magnets and collimators selects positively charged particles with 75 GeV/c momentum; this secondary beam is composed of 6% of K^+, 71% of π^+ and 23% of protons, with a total rate of 750 MHz. Charged kaons are positively identified by a Cherenkov detector (KTAG) and their momentum is measured by a silicon pixel detector (GigaTracKer or GTK) composed of three stations interspersed by two pairs of dipole magnets. The kaon decay region is a 60 m long vacuum vessel equipped with Large Angle Veto (LAV) detectors made of lead glass blocks. A magnetic spectrometer with Straw Chambers measures the momentum of charged tracks from kaon decays; this detector is composed of 2+2 stations placed in vacuum before and after a dipole magnet which produces a momentum kick of

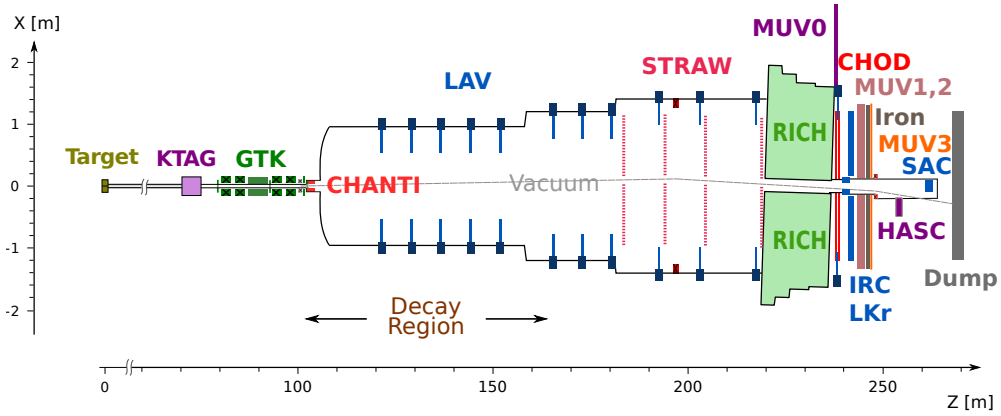

Figure 1. Layout of the NA62 experiment.

270 MeV/c. An electromagnetic (e.m.) calorimeter filled with Liquid Krypton (LKr) is used to detect and identify electrons and photons from kaon decays and is followed by hadron calorimeters and small angle e.m. calorimeters. A RICH detector to distinguish muons from charged pions is located between the end of the magnetic spectrometer and the LKr. A scintillator hodoscope (CHOD), located just downstream of the RICH, is used to measure the crossing time of charged particles and produce a L0 trigger signal. Upstream inelastic interactions are vetoed by the CHANTI detector placed after the third station of GTK. Details of the NA62 apparatus can be found in [2] and a view of the NA62 experiment layout is shown in figure 1.

2 RICH detector

The main background to the signal $K^+ \to \pi^+\nu\bar{\nu}$ is the decay $K^+ \to \mu^+\nu_\mu$, which has a branching ratio of 63.5%, about 10 orders of magnitude larger than the signal. The suppression of this background is achieved by kinematic methods and by using the very different stopping power of muons and charged pions in the calorimeters. A further factor 100 of suppression is obtained by means of a Cherenkov detector, the RICH. The momentum fiducial region over which pion-muon separation is required extends between 15 and 35 GeV/c; the separation is most effective if the lower bound is close to the Cherenkov threshold of the radiator. Neon at atmospheric pressure, chosen as a radiator for the RICH, has the refractive index $n = 1 + 62.8 \times 10^{-6}$ at a wavelength $\lambda = 300$ nm, corresponding to a charged pion Cherenkov threshold of 12.5 GeV/c. Neon has also many other useful characteristics, like a good light transparency and a low chromatic dispersion. On the other hand, the very small value of $(n - 1)$ implies that very few photons are produced per unit track length so a long radiator volume is needed. Two prototype detectors were built and tested in hadron beams to demonstrate the performance of the proposed layout: the results of these tests have been published [3, 4].

The RICH neon container ("vessel") is a vacuum proof tank 17 m long, made of steel and composed of 4 cylindrical sections of decreasing diameter (the most upstream one is about 4 m large) closed by two thin aluminium windows to minimize the amount of material crossed by incoming/outgoing particles. A steel conical cap connects the upstream window with the first cylindrical section and accommodates the light sensors (photomultipliers, PMTs) placed outside

2017 JINST 12 P12017

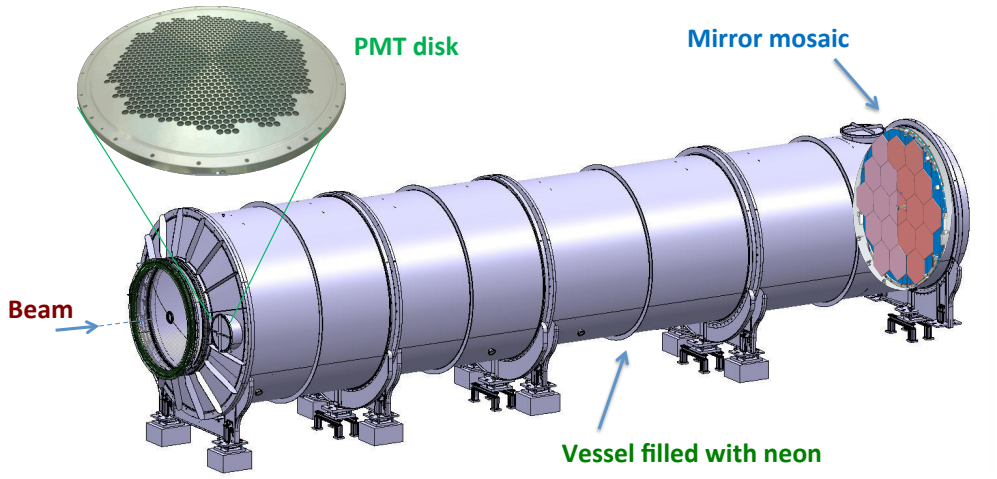

Figure 2. The RICH detector. The hadron beam enters from the left and travels in vacuum through a beam pipe which crosses all the detector. A zoom on one of the two disks accommodating the light sensors (photomultipliers, PMTs) is shown on the left; the mirror mosaic inside the neon container ("vessel") is visible on the right.

the particle acceptance in two disks containing 976 PMTs each. A schematic view of the RICH detector is shown in figure 2.

A beam pipe, 168 mm in diameter, crosses all the length of the RICH detector to allow undecayed particles to travel in vacuum down to the experiment beam dump.

The total neon volume is about 200 m^3: fresh neon is injected inside the container after it has been fully evacuated, then sealed. No purification or recirculation system is present.

3 Mirrors

A mosaic of spherical mirrors is used to transform the Cherenkov light cone into a ring in the mirror focal plane. The total reflective surface exceeds 6 m^2 and, thus, it is practical to use a matrix of 20 mirrors. The NA62 RICH detector uses spherical mirrors with a nominal curvature radius of 34 m and hence a focal length of 17 m. In order to avoid the absorption of the reflected light by the beam pipe, the mirrors are divided into two groups with different orientation of the spherical surfaces, one with the centre of curvature located to the left and the other to the right of the beam pipe. Out of the 20 mirrors needed, 18 have hexagonal shape (35 cm side dimension) and 2 a semi-hexagonal one. These last two are used in the centre of the mosaic and have a semi-circular hole on one side in order to accommodate the beam pipe. Each mirror is made of 2.5 cm thick glass, coated with aluminium on the optically machined surface; a dielectric film is added in order to protect the aluminium layer from oxidation, see sub-section 3.3. Each hexagonal mirror has a blind hole close to its barycentre in the rear surface where an aluminium dowel is inserted to support the mirror itself; two other blind holes are needed for the installation procedure as described in section 6. The semi-hexagonal mirrors have two blind holes for two dowels. The orientation of each mirror is performed by thin aluminium ribbons attached on the rear surface and connected to piezo-electric motors. A view of

2017 JINST 12 P12017

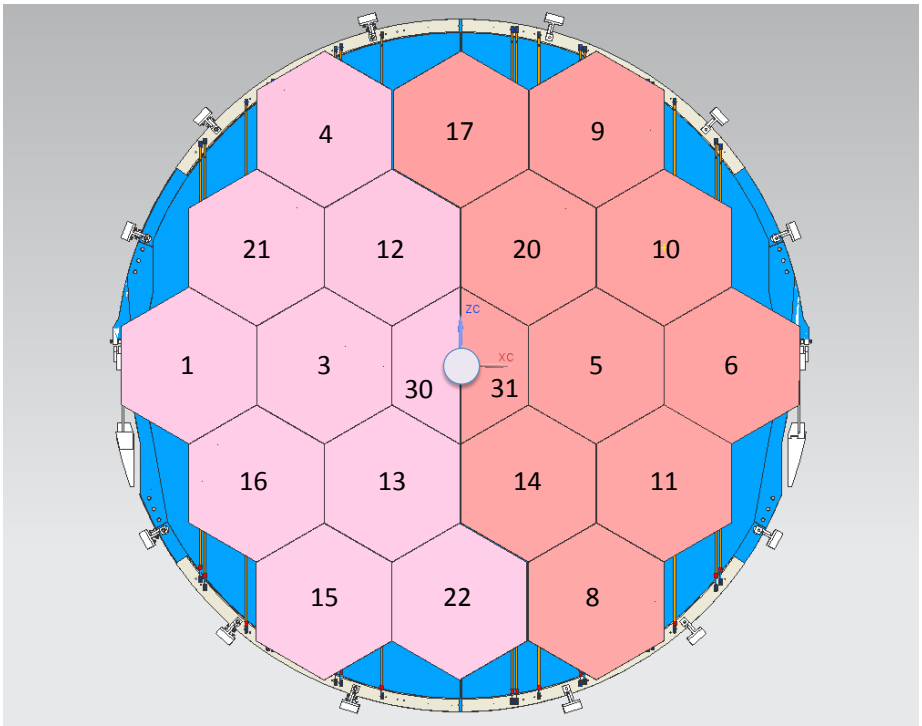

Figure 3. Front view of the mosaic of 18 hexagonal and two semi-hexagonal mirrors; the support panel and some of the aluminium ribbons are visible behind the mirrors. The different colours represent mirrors pointing to the left or to the right of the beam pipe which crosses the centre of the mosaic; numbers indicate manufacturing order.

the mirror mosaic is shown in figure 3, details of a hexagonal and two semi-hexagonal mirrors, seen from the rear part, are shown in figure 13. The mirror support system is described in section 4.

The hexagonal mirrors must fulfil the following geometrical requirements:

- a hexagonal shape inscribed in a circle of diameter 70.0 ± 0.1 cm;
- two blind holes, 1.2 cm diameter and 1.5 cm deep, in the rear surface, at a distance of 56.0 cm one from the other, symmetrical with respect to the mirror centre;
- one blind hole, 1.2 cm diameter and 1.5 cm deep, in the rear surface in the centre of the mirror.

The two semi-hexagonal mirrors must have:

- a semi-hexagonal shape obtained by cutting an hexagon inscribed in a circle of diameter 70.0 ± 0.1 cm;
- a semi-circular hole of diameter $18.0^{+0.1}_{-0.0}$ cm in the middle of the longest side;
- two blind holes, 1.2 cm diameter and 1.5 cm deep, in the rear surface, at a distance of 8.0 cm from each other.

2017 JINST 12 P12017

Each of the mosaic mirrors must satisfy three optical criteria:

- a D_0,[1] not larger than 4 mm;
- actual focal length within ±10 cm from the nominal one;
- an average reflectivity, in the wavelength range between 200 and 600 nm, at about 90%.

In total, 21 mirrors were manufactured by Marcon[2] (19 hexagonal and 2 semi-hexagonal, one hexagonal mirror being a spare). The optical quality parameters mentioned above were measured for each mirror before installation. The measurements are described in sub-section 3.2.

During the 2015-2016 winter shutdown the semi-hexagonal mirrors and their support pins were replaced with two pre-series semi-hexagonal mirrors made by Marcon in 2009, with the same focal length and optical quality as the series ones, but with slightly different dimension and position of the blind holes for the support and of the semi-circular hole.

3.1 Geometry measurement

The dimensions of the mirrors manufactured by Marcon were measured using a coordinate measuring machine (DEA CMM) with a nominal measuring accuracy of 0.01 mm. The main result of the measurement is that the hexagonal mirrors are slightly squeezed, with the distance between the vertical sides smaller than that between the oblique sides by about 1.5 mm (mirrors are oriented as in figure 3); the vertical sides are longer than the oblique sides by about 1.5 mm too. Defining a horizontal line passing through the mirror barycentre as the x axis, with the y axis vertical, the design position of the central blind hole is $y = -3$ mm, while the outer blind holes are tangent to the x axis ($y = -6$ mm). In addition to the geometry of the mirrors, the position of the blind holes were measured. Overall the geometry precision fits the requirements.

3.2 Optical quality measurement

From the optical theory it is known that if a point like source is put in the centre of curvature of an ideal spherical mirror, with a radius of curvature R and focal length $f = R/2$, all the incident light is cast back to the centre of curvature. This can be easily obtained from the conjugate points law $1/p + 1/q = 1/f$, where p and q are the distance of the source and of the image, respectively, from the mirror. A real mirror, on the other hand, casts back an image that is not point-like, but of a finite size. Measuring the image profile it is possible to quantify the optical quality of the mirror itself: in particular the parameter D_0 is to be measured. Assuming that the transverse distribution of the light intensity is a two-dimensional gaussian with standard deviations σ_x and σ_y, it can be shown that

$$D_0 = \sqrt{8 \ln \frac{1}{0.05}}\, \sigma \approx 4.9\sigma \tag{3.1}$$

where $\sigma = \sqrt{\sigma_x \sigma_y}$. To measure the optical parameters a laser (Helium-Neon laser, 632.8 nm light emission, Uniphase 1122P) with a converging lens (focal length 6 cm) was placed on a table at a

[1] D_0 is the diameter of the smallest spot image of a point source placed in the mirror curvature centre, where 95% of the light is collected.

[2] MARCON Costruzioni Ottico Meccaniche, via Isonzo 4 — 30027 San Donà di Piave (VE) Italia (http://www.marcontelescopes.com/).

2017 JINST 12 P12017

distance of about 34 m from a support where one mirror at a time was positioned. Thanks to this lens it was possible to produce a point source and to illuminate almost all the mirror. On the same table of the laser a photodiode to detect the reflected light was placed together with a blade. The blade support, independent of the photodiode, allowed micrometric movements along the vertical (y) and horizontal (x) transverse directions (perpendicularly to the direction of propagation of the reflected light) and also along the laser light direction (z axis). The support was moved from a fixed reference z point in search of the position of minimum transverse size of the image. For each value of z, the distribution of the amount of light collected by the photodiode was measured as a function of the transverse (x or y) coordinate of the blade that was moved along the corresponding axis. Fitting these distributions with the sum of an error function and a constant, σ_x and σ_y were determined for each z position. Measuring the distance d_{LM} between the point source and the mirror, the distance d_{BM} between the blade in the reference position and the mirror and the displacement Δz_{min} between the reference point and the blade position corresponding to the smallest image size, the focal length could be calculated:

$$f \equiv \frac{d_{LM} + d_{BM} - \Delta z_{\text{min}}}{4} \tag{3.2}$$

where Δz_{min} is positive towards the mirror; d_{LM} and d_{BM} were measured with a telemeter, Δz_{min} was obtained by fitting with a second-order polynomial σ vs z, z being the blade position measured by the micrometric support. The same kind of measurements was also performed for the semi-hexagonal mirrors. The light spot produced by the converging lens was larger than a semi-hexagonal mirror, so the lens was removed and the direct light from the laser was used, resulting in a smaller spot size on the mirror (in this case the laser source was not exactly a point source). In order to have information about the spatial uniformity of optical parameters, the same measurements in this configuration were performed for three different points for each semi-hexagonal mirror.

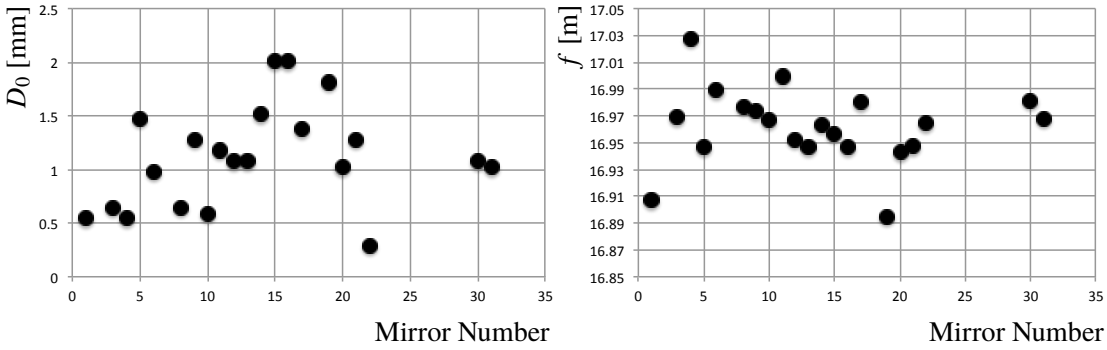

Figure 4. Measurement of the mirror optical parameters, see text for details. The numbering is the same as in figure 3.

The results obtained are shown in figure 4 (for the semi-hexagonal mirrors the average of three measurements is shown), where mirrors are identified by the same numbers as in figure 3. The semi-hexagonal mirrors correspond to number 30 and 31. D_0 values are below 2.5 mm for all mirrors and thus fit the requirements. The focal length, furthermore, ranges between 16.907 m and 17.028 m, so there is a difference of maximum 12 cm between two different mirrors, which fulfils the requests.

2017 JINST 12 P12017

3.3 Aluminization and reflectivity measurement

The requirements for the NA62 RICH detector mirror system have been a high ($\approx$ 90%) and uniform reflectivity in the range of 200 nm - 600 nm. Since the Cherenkov photon density is higher at low wavelength ($dN/d\lambda \approx 1/\lambda^2$), the main focus has been given to the UV part of the spectrum. Standard solution for thin film technology for reflective coatings are thin metal layers, see figure 5.

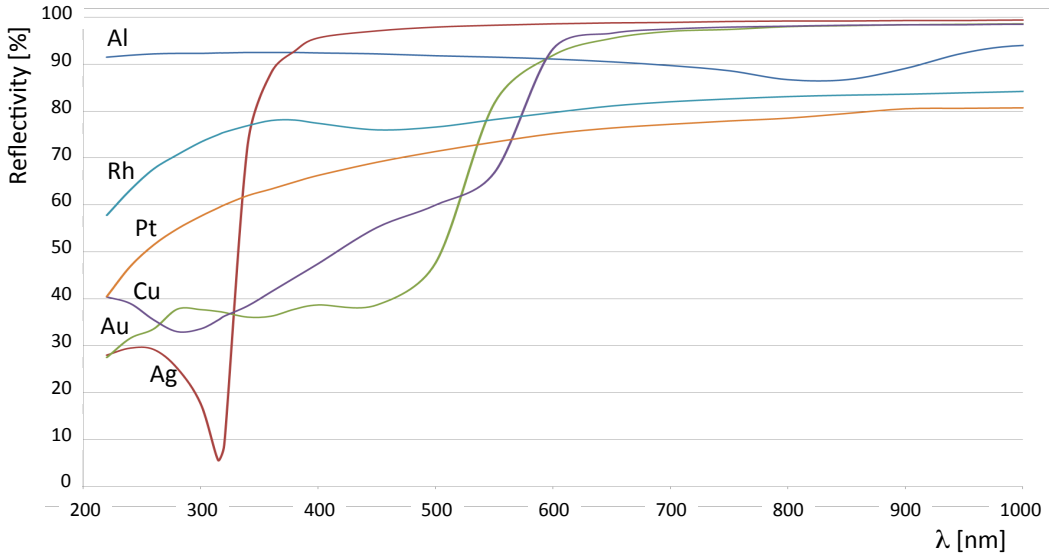

Figure 5. Reflectivity for different thin metal layers as a function of wavelength λ in nm.

Looking at the different metals Aluminium is the best candidate for a uniform reflectivity in this wavelength range. On top of the reflective layer a protective transparent dielectric layer is needed. A special recipe with Aluminium (Al) and Magnesium Fluoride (MgF_2) has been developed in the Thin Film and Glass service at CERN to provide good and uniform performance without losses in the far UV range. Standard mirror coatings with Aluminium and Quartz (SiO_2) have worse performance in the UV range, see figure 6.

Another important consideration for a 'state of the art' coating is the attachment performance of the layer system to the glass substrate. Chromium has much better attachment properties to glass than Aluminum. Therefore as a first step a very thin ($\approx$ 10 nm) attachment layer of Chromium is applied to the substrate before the reflective and protective layers. The recipe for the RICH mirrors has been:

- 10 nm Chromium for a better attachment;
- 90 nm Aluminium for a uniform and high reflectivity;
- 31 nm of Magnesium Fluoride as a protective layer.

19 hexagonal mirrors and 2 semi-hexagonal mirrors have been coated in 2014 at CERN. Only the reflective side of mirrors was coated. For each mirror a custom support has been constructed for a better handling during production and final stocking. The $\approx$ 20 kg heavy glass substrates passed through a standard cleaning procedure with soap, water, distilled water and extremely pure ethilic

2017 JINST 12 P12017

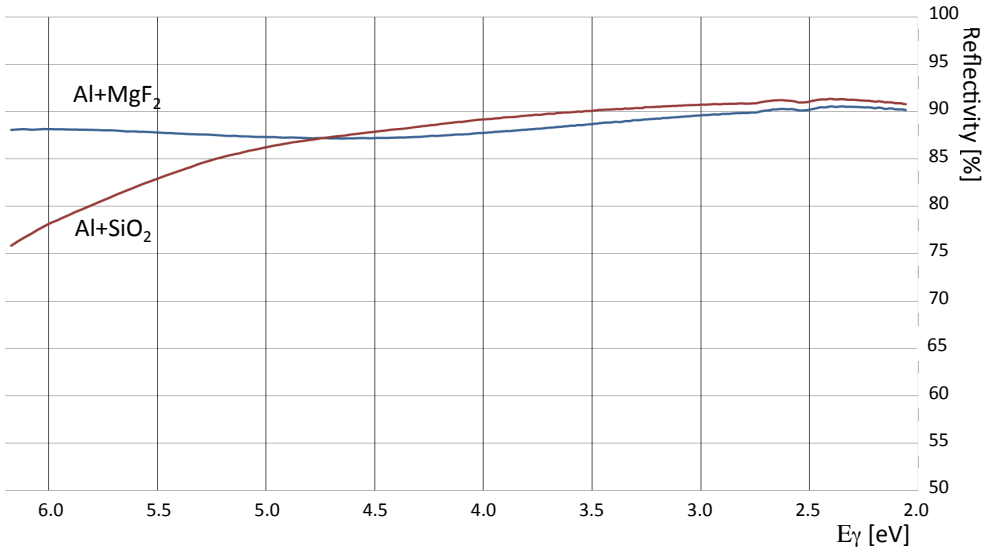

Figure 6. Total reflectivity for two different coatings as a function of photon energy.

alcohol. The remaining alcohol was then dried with the help of compressed nitrogen jets to avoid any cleaning traces. The cleaned substrate was then carefully positioned on the round turning plate. 3 fixation pieces on the edges prevented falling and 3 V-pieces in the corners avoided rotation. The plate including substrate was turned upside down and then fixed to the rotation mechanics in the evaporator. After about 1 day pumping time, reaching a vacuum of the order of 10^{-7} mbar the coating process has been performed. Removed from the coater a careful visual inspection of the coating result was performed. The substrate was then positioned with the reflective face upside down and fixed in a holding frame and sealed in a nitrogen filled plastic bag for final storage until installation.

The quality control reflectivity scan of the reference samples of each mirror coating has been performed with the Universal Reflectivity Accessory of a LAMBDA 650 Perkin Elmer spectrometer. Very good uniformity in the order of ±1% over the whole production has been reached, see figure 7.

4 Mirror support and orientation system

The mirror system is supported by an aluminium honeycomb panel (support panel), placed inside the vessel in front of downstream end-cap. The mirror surfaces lay on two spheres with different x coordinates of the centre and the same radius of curvature of 34 m. The panel is divided into two halves and is designed to support 400 kg load of the mirror mosaic, but, at the same time, to be as transparent as possible to high energy photons and electrons to be detected by the downstream LKr calorimeter. Each mirror is individually supported and adjustable for alignment.

4.1 Support panel

The support panel, manufactured by CINEL,[3] is a structure of 3 m in diameter, divided in two halves along the vertical axis (figure 8-left). The two halves can be oriented, at the time of the installation,

[3]CINEL Strumenti Scientifici s.r.l, via dell'Artigianato, 14, Vigonza, Italy.

2017 JINST 12 P12017

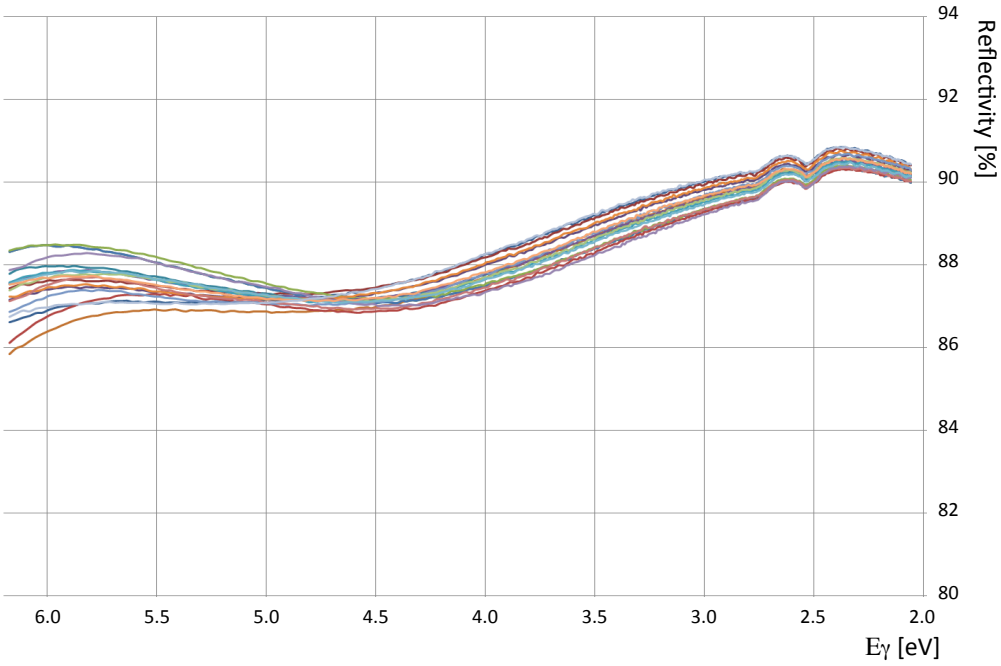

Figure 7. Reflectivity as a function of photon energy; each line represents a single mirror.

toward the left and right side of the beam pipe, i.e. the corresponding locations of the two flanges that house, at the opposite side of the vessel, the PMs. The panel, a honeycomb structure of 5 cm total thickness, is made of an aluminium honeycomb core placed between two aluminium layers 1 mm thick each. The chosen material allows to have robustness of the structure and, at the same time, provides reduced material budget for crossing particles, for a total of 5% X_0. Holes were made to allow the crossing from the back to the front of the panel of some mechanical parts needed for the mirror installation. The mechanical processing of all parts (position of the feedthrough holes, service holes, etc) was done with a precision of 0.1 mm; this required precision is uniform on the whole surface of the panel. The support panel is connected to the vessel by means of a stiffening aluminium flange (figure 8-right). Two blocks at mid height (one for each side), attached to the inner part of the vessel, bear the panel weight; 12 small blocks, all around the structure, are connected to the vessel wall and are used to align the panel in the final position. The mirrors are installed on the panel through a mechanical interface system composed of: a mirror support, which includes a pin (dowel) directly in contact with the mirror and a conical structure housing the pin, two stabilizing ribbons to keep the mirror in equilibrium and to allow its orientation, and one anti-rotation ribbon to avoid the rotation of the mirror around the pin axis.

4.2 Single mirror support

Each mirror is individually sustained at a single point by means of a pin (dowel) inserted in a blind hole drilled in its rear face for this purpose, and attached to an intermediate structure (support) positioned on the panel. After a careful simulation of the shear strength due to the weight of the mirror, it turned out that the best choice for the shape of the support was a truncated cone, hollowed out in its internal part; in this way, also the material budget was minimized. A total

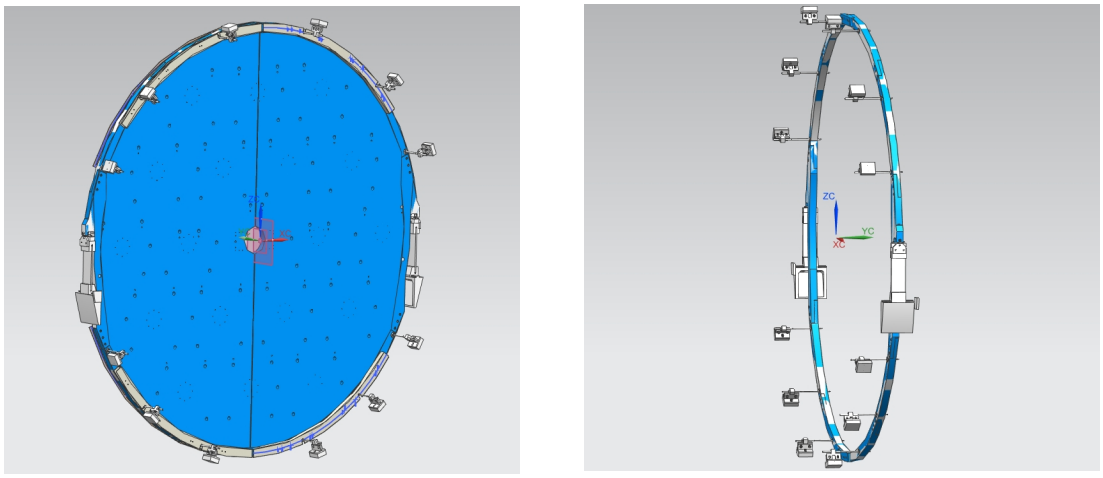

Figure 8. Left: overall front view of the mirror support panel; the honeycomb panel (blue) is divided in two halves. Right: view of the stiffening aluminium flange (the honeycomb panel has been removed for clarity) connecting the support panel with the RICH vessel; the blocks at mid height on both sides bear the panel weight and are supported by the inner part of the RICH vessel; the 12 small blocks all around the panel are connected to the vessel wall to proper align the panel.

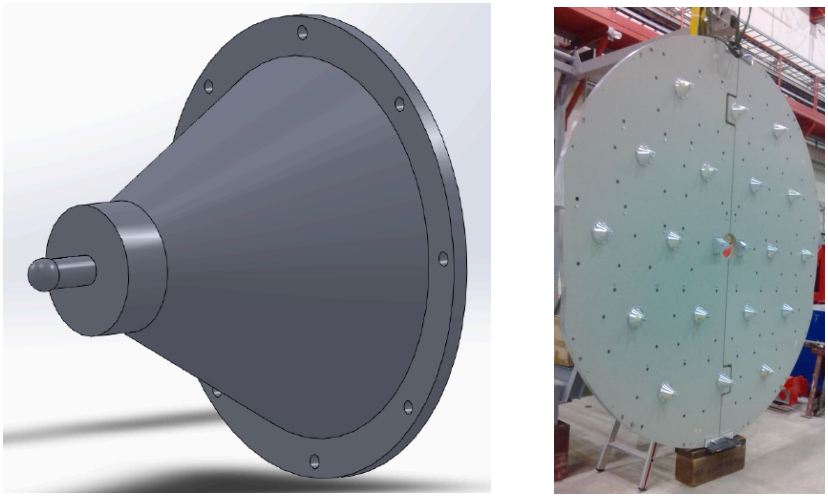

Figure 9. Left: drawing of one dowel holding aluminium cone for mirror support. Right: support panel with all the cones mounted, before installation in the RICH vessel.

of 18 truncated cones, needed for the hexagonal mirrors, have been manufactured in the Perugia University mechanical workshop. In order to cope with the spherical surface of the mirror mosaic, the truncated cones have all the same aperture, but different heights. Figure 9-left shows a picture of one cone with the dowel inserted. All the cones were mounted on the panel before its installation inside the vessel. A picture of the panel with all the cones in their position is shown in figure 9-right. The supports for the two semi-hexagonal mirrors have different shapes and functionality.

The position of the mirror hanging point is slightly below its centre of mass; therefore, the mirror is free to rotate along the x and y axes and tends to fall in the forward direction. In order to

2017 JINST 12 P12017

avoid the falling and to keep the mirror in equilibrium, two aluminium ribbons, each connected to a piezo-electric motor, are attached to two pins placed on its back. In this way the mirror weight can be used to maintain the ribbon tension and to modify the mirror orientation simply pulling or releasing the ribbon. In addition, a third aluminium ribbon is used to avoid rotation around the azimuthal angle. The pins, made of stesalite, were glued on the rear surface of the mirrors after the aluminization process of the front surface was completed. Gluing was done in a clean room, using epoxy glue and dedicated jigs, designed and manufactured to precisely position the pins with respect to the mirror geometry. After the gluing procedure, the mirrors were stored in a safety case to protect their surfaces and to facilitate their transport. The support system of the two semi-hexagonal mirrors is different with respect to the hexagonal ones. For each mirror an aluminium pyramid attached to the support panel (see figure 10-left) houses the two dowels that are inserted in the two blind holes during the mounting. One of these dowels has the possibility to be moved along the vertical axis while the other can be moved along the longitudinal direction (parallel to the axis of the RICH vessel and perpendicular to the surface of the mirror support). The fall of the mirror has been avoided by a single aluminium ribbon connected to a piezo-electric motor, the rotation of the two mirrors is already avoided by the presence of two dowels, so no anti-rotation ribbon is installed in this case (see figure 10-right). These three degrees of freedom allow the alignment of the two semi-hexagonal mirrors during their mounting procedure. Given that the movements of the two dowels of each mirror are possible only when the pyramids are directly accessible, the only movement allowed after the closure of the vessel is the one given by the ribbon connected to the piezo-electric motor. Due to such limitation, the only alignment procedure possible for the semi-hexagonal mirrors is the one with the laser when the vessel is still open, see section 7. Then, once the vessel has been closed, the two semi-hexagonal mirrors have been chosen as reference mirrors for the corresponding set of mirrors (left and right) and afterwards all the mirrors have been aligned remotely with respect to the corresponding semi-hexagonal mirror.

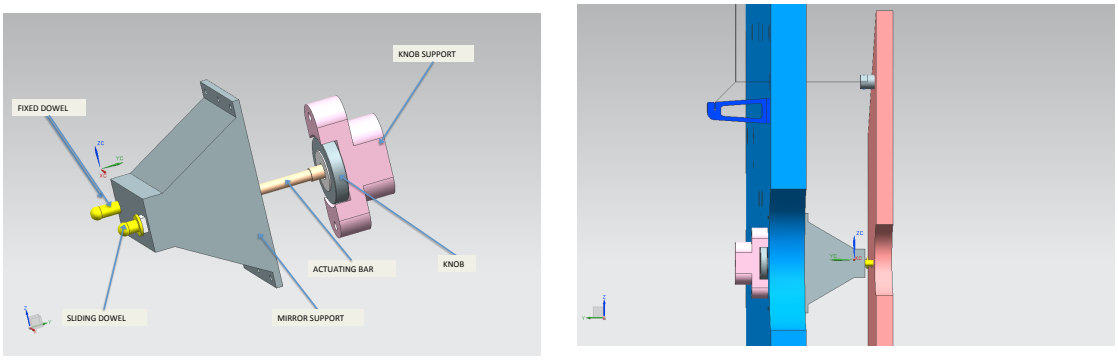

Figure 10. Left: the support pyramid for the semi-hexagonal mirror; one dowel can be advanced manually during installation, with the help of knob support (pink), which is then removed, allowing the orientation in the horizontal direction. After installation only the vertical orientation can be remotely adjusted. Right: one semi-hexagonal mirror in place: the honeycomb support panel is in blue, the mirror in orange, the support pyramid in grey, the dowel in yellow; the stabilizing ribbon can also be seen.

2017 JINST 12 P12017

4.3 Stabilizing and anti-rotation ribbons

The ribbons, manufactured by Lamineries Matthey,[4] are made of aluminium Anticorodal 110, AW-6082, are 200 μm thick and 10 mm wide. Three ribbons are needed for each hexagonal mirror, a single ribbon for each semi-hexagonal one. Due to the different positions of the mirrors on the panel, all the ribbons are cut individually at different lengths, according to the mirror location. The anti-rotation ribbon runs along the front part of the panel (see figure 11-left), each of the two stabilizing ribbons runs along the rear part of the panel (see figure 11-right). One end of each stabilizing ribbon is attached to the corresponding piezo-electric motor fixed on a support bar (U-bar) by means of an adjustable screw, used for tensioning of the ribbon and for rough positioning of the mirror. The fine positioning is performed using the piezo-electric motors. The other end is connected to the mirror by means of an arrangement, shown in figure 12, that allows the transmission of the movement from the piezo-electric motor to the mirror itself, by turning the pulling force exerted by the motor from vertical to horizontal. The positions of the ribbon attachment on the mirror are shown in figure 13-left (hexagonal mirrors) and in figure 13-right (semi-hexagonal mirrors). The location of the ribbons with respect to the mirrors can be seen in figure 14.

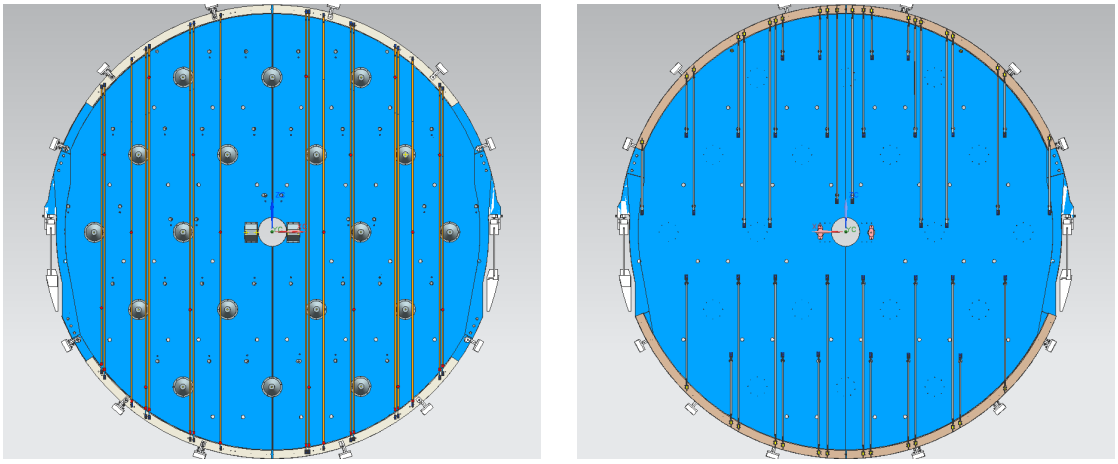

Figure 11. Left: front view of the anti-rotation ribbons and mirrors support cones. Right: rear view of the stabilizing ribbons.

4.4 Piezo-electric motors

A precise orientation of each mirror is achieved by means of piezo-electric motors.[5] These motors have a ±35 mm travel range with 1 nm step and can produce up to 20 N of push/pull force. These devices are self-locking and remain in the same position if the supply voltage is turned off. The motor is split in an upper and a lower part, with a ceramic rod sliding in between; the bulk of the motor is fixed to the support panel structure, the ceramic rod is connected to the aluminium ribbon. On top of the motor upper part an encoder is mounted to check precisely the position of the rod; a U-shaped aluminium frame is fixed at both ends of the motor ceramic rod and contains a magnetised scale which is located in front of the encoder sensor. Limit switches guarantee that the ceramic rod

[4]Lamineries Matthey SA, Rte de Neuchâtel, Case postale CH-2520 La Neuville, Switzerland, www.matthey.ch.
[5]Type LEGS-LT02SV-10 produced by PiezoMotor Uppsala, Sweden.

2017 JINST 12 P12017

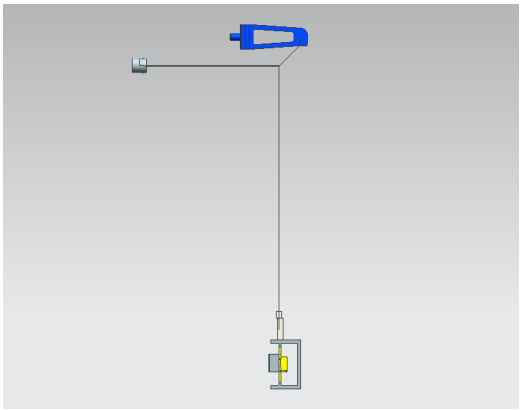

Figure 12. Transmission tool with a stabilizing ribbon; on the bottom a piezo-electric motor is shown. The tool (blue) which turns the ribbon from vertical to horizontal is attached to the not shown support panel. On the left the stesalyte cylinder, glued to the mirror rear part, is shown.

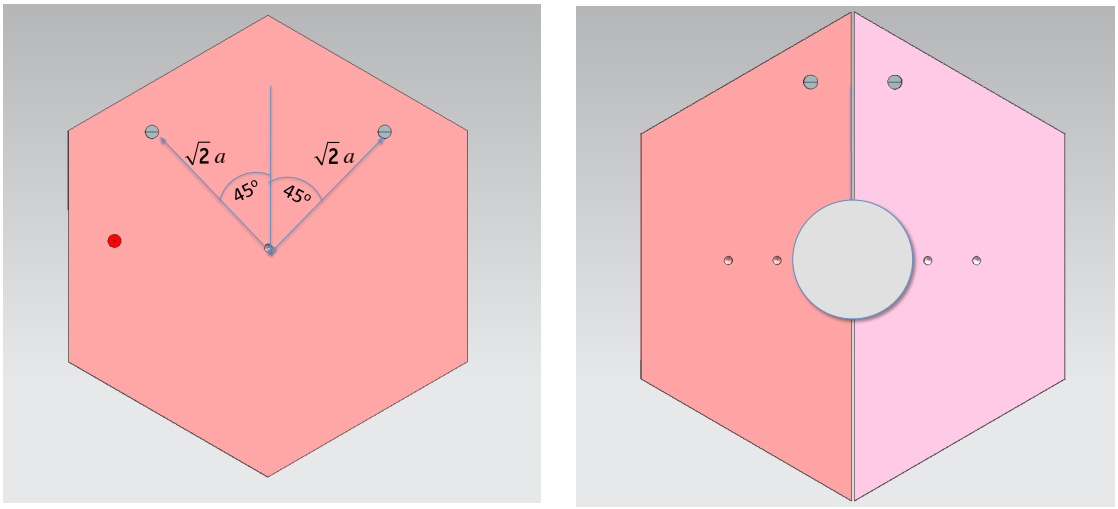

Figure 13. Positions of the ribbon attachment for hexagonal (left) or semi-hexagonal (right) mirrors (gray for stabilizing ribbons, red for anti-rotating ribbon). View from the mirror rear side. For the meaning of the parameter a, see section 5.

remains within the allowed range. A detailed view of a piezo-electric motor assembly is shown in figure 15-left. All the motors are located outside particle acceptance. Figure 15-right shows three piezomotors installed on the U-bar frame.

The motor movement is remotely controlled by a custom-made electronic board, which contains a single micro-stepping driver which is connected to the motor to be moved; the board is connected via USB to a PC where a control program runs. The program selects a motor, sets the movement velocity, the direction and the travel length to be achieved, controlled by the associated encoder. The control board and the dedicated PC are located near the RICH detector and the movement program can be run remotely from the experiment control room. Each hexagonal mirror is oriented by two motors, each semi-hexagonal mirror by a single motor, for a total of 38 motors.

2017 JINST 12 P12017

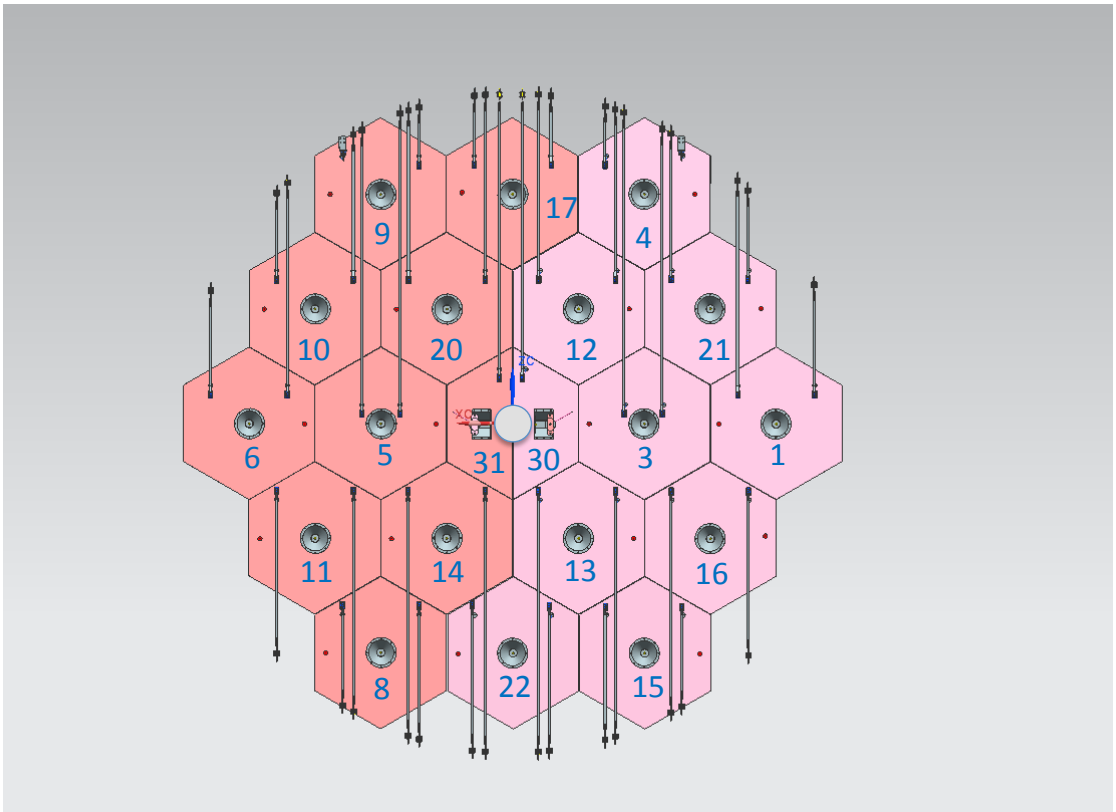

Figure 14. Rear view of the mirror mosaic with connected stabilizing ribbons. Red points correspond to the attachment position of anti-rotation ribbons. Two stabilizing ribbons (mirror 9-left and mirror 4-right) do not use the transmission, see also figure 15.

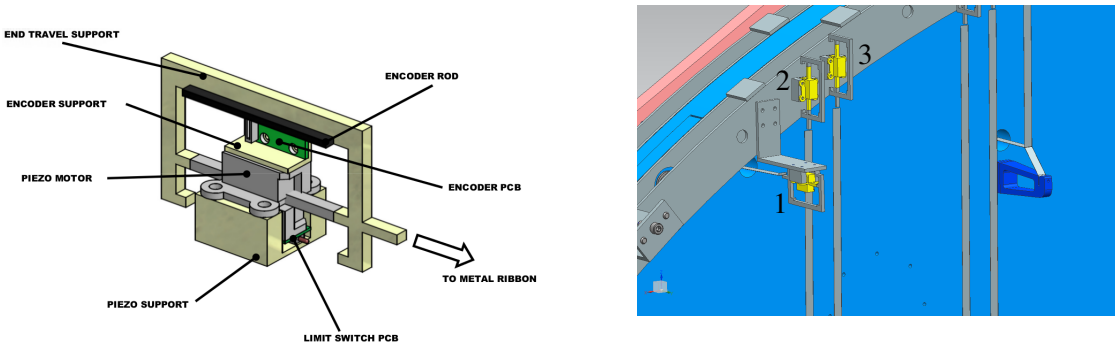

Figure 15. Left: view of a piezo-electric motor. Right: view of three piezo-electric motors (in yellow) on the frame. Motors 2 and 3 are oriented vertically and use the transmission tool (one connected to a different motor is shown in blue), while motor 1 is oriented horizontally and is directly connected to the mirror.

5 Relation between piezo-electric motors movement and mirror orientation

In this section a simple model relating the movements of two ceramic rods (each one attached to a corresponding piezo-electric motor) and the change in the mirror orientation is developed. The starting orientation of an hexagonal mirror is defined to be vertical. A local coordinate system is

2017 JINST 12 P12017

defined with the y axis vertical, the x axis horizontal and parallel to the mirror surface, the z axis horizontal and perpendicular to the mirror face. The origin O of the axes is the touching point of the dowel on the inner surface of the mirror rear blind hole, at a distance d from the blind hole centre. The barycentre G is upstream by a quantity b (about 3 mm) and below O by a quantity c. The stabilizing ribbons are joint on the mirror rear surface at a distance $\sqrt{2}a$ from the blind hole centre at $\pm 45^o$ from the vertical; the two joint points are called A and B. For simplicity the piezo-electric motors are assumed directly pulling the mirror, both at distance l from the mirror; point P is the position of the motor pulling the ribbon attached in A, point Q corresponds to B. In summary the starting conditions are (see section 3.1 for details and also figures 12 and 13):

$$\begin{aligned} O &= (0,0,0)\,, & G &= (0,-b,+c)\,, \\ A &= (+a,+a,-d)\,, & B &= (-a,+a,-d)\,, \\ P &= (+m,+n,-p)\,, & Q &= (-m,+n,-p)\,. \\ |P-A| &= |Q-B| = l \end{aligned} \tag{5.1}$$

Rotations are defined with respect to point O, labelled by the rotation axis. To first order in the rotation angles θ_X, θ_Y and θ_Z, the rotation matrix R is:

$$R = \begin{pmatrix} 1 & \theta_Z & -\theta_Y \\ -\theta_Z & 1 & \theta_X \\ \theta_Y & -\theta_X & 1 \end{pmatrix} \tag{5.2}$$

The points A' and B' are the new positions of the ribbon joints on the mirror after the rotation:

$$(A'-O) = (A-O) + (\theta_Z a + \theta_Y d, -\theta_Z a - \theta_X d, \theta_Y a - \theta_X a), \tag{5.3}$$
$$(B'-O) = (B-O) + (\theta_Z a + \theta_Y d, \theta_Z a - \theta_X d, -\theta_Y a - \theta_X a), \tag{5.4}$$

Assuming that the rotation is induced by a movement of motors by Δl_A and Δl_B respectively, to first order the new relations are:

$$|P-A'|^2 = l^2 + 2l\Delta l_A, \tag{5.5}$$
$$|Q-B'|^2 = l^2 + 2l\Delta l_B. \tag{5.6}$$

and using (5.3) and (5.4):

$$-a\,(m-n)\,\theta_Z + (nd-ap)\,\theta_X + (pa-md)\,\theta_Y = l\Delta l_A \tag{5.7}$$
$$+a\,(m-n)\,\theta_Z + (nd-ap)\,\theta_X - (pa-md)\,\theta_Y = l\Delta l_B \tag{5.8}$$

The angle θ_X is unambiguously determined (it is the the rotation "falling" with gravity), while θ_Y and θ_Z are linearly correlated:

$$\theta_X = \frac{l\,(\Delta l_A + \Delta l_B)}{2\,(nd-ap)}, \tag{5.9}$$
$$-a\,(m-n)\,\theta_Z + (pa-md)\,\theta_Y = \frac{l\,(\Delta l_A - \Delta l_B)}{2} \tag{5.10}$$

2017 JINST 12 P12017

We notice that θ_Z is unconstrained if $m = n$. Here the stabilizing ribbon enters: it prevents a rotation on the z axis so we can assume $\theta_Z = 0$; we also take $m = n = a$

$$\theta_X = \frac{l\,(\Delta l_A + \Delta l_B)}{2a\,(d - p)}, \tag{5.11}$$

$$\theta_Y = \frac{l\,(\Delta l_A - \Delta l_B)}{2a\,(p - d)} \tag{5.12}$$

and finally, noting that, from 5.1, $l = p - d$ we have

$$\theta_X = -\frac{(\Delta l_A + \Delta l_B)}{2a}, \tag{5.13}$$

$$\theta_Y = \frac{(\Delta l_A - \Delta l_B)}{2a} \tag{5.14}$$

For most of the hexagonal mirrors $\sqrt{2}a \approx 250$ mm, so if both motors of a mirror move by, say, 10 μm, $\theta_X \approx 60$ μrad and $\theta_Y = 0$.

6 Mirror installation

The installation process started with the preparation of piezo-electric motors supports. The piezo-electric motors were mounted on four circular shaped U-bars, installed at the edges of the support panel in its rear part, in positions top-right, top-left, bottom-right, bottom-left. The U-bars served as rails to house the electric cables used to power and control the piezo-electric motors. Once the support panel and the U-bars were installed inside the vessel in their final positions, a SAS (Safety Access System) was mounted at the downstream end of the vessel in order to access the backside of the support panel preserving a clean environment. At the upstream end of the vessel a structure for the laser mirror alignment was mounted. A removable plastic sheet was used to close the upstream side of the vessel, once all the material needed for the mirror installation had been introduced inside the vessel. The access to the vessel was granted by a service hole, equipped with a second SAS, placed in the third downstream section of the vessel. During the mounting operations, clean air was flushed through the downstream SAS; in addition, oxygen and humidity levels were steadily measured inside the vessel.

Figure 16. Left: installation tool with a hexagonal mirror ready to be mounted. Right: mirror mosaic close to completion (only two hexagonal mirrors on the top right are missing; the installing tool is visible on the left.

2017 JINST 12 P12017

Before starting the mirror mounting, the position of each dowel was measured by the CERN metrology service with respect to the experiment reference frame. Such positions were introduced in a template drawing reproducing the support panel and all the mirrors (with their measured sizes), in order to anticipate possible mechanical conflicts among the mirrors (during the design of the support panels and the aluminium cones the clearance between mirrors edges was kept to 1 mm). The installation of the mirrors proceeded from the bottom raw to the top one, in order to have always the top part of each mirror free and accessible from the front side of the support panel. A temporary platform was mounted in front of the support panel (at a distance of 40 cm) with a maximum height of 50 cm, to facilitate the installation procedure. Later on, to install the top two rows of mirrors, a second platform was placed on top of the first one reaching a maximum height of 150 cm. The mirrors were transported inside the vessel and installed in their final position one by one. Each mirror, once inside the vessel, was extracted from its hermetic bag, released from the safety case and put in vertical position using special tongs, designed and manufactured on purpose. Such tongs were blocking the mirror exploiting two service blind holes placed on the rear side of the mirror and its lateral surfaces. The tongs were then hung to a mechanical arm with three degrees of freedom (the x, y and z positions were adjustable with three toothed pulleys) mounted on the top of a trolley with 4 wheels allowing further movements, see figure 16. The trolley was moved in front of the support panel and, by adjusting the three toothed pulleys, the position of the mirror was fine-tuned in order to place its blind hole just in front of the corresponding dowel, fixed to the support panel, and deliver the mirror. In order to avoid crashes during this operation a spacer was introduced between the back of the mirror and the surface of the cone where the dowel was mounted. Once the mirror was in the correct position, two safety pins were introduced, through dedicated service holes, into the support panel in contact with the rear surface of the mirrors, in order to avoid their fall after the removal of the tongs and before connecting the stabilizing ribbons. The stabilizing ribbons coming from the back of the support panel were attached to the corresponding stesalite pins with a screw, accessing the back of the mirror from its top. The anti-rotation ribbon was fixed to its corresponding pin on the mirror with a screw accessible from another service hole present in the support panel.

7 Laser alignment of RICH mirrors

Each half of the RICH mirror mosaic is designed to reflect light as a single spherical mirror. The orientation of the half-mosaic with respect to the PMT flanges, defined by the position of its centre of curvature, is chosen in order to maximise the detector acceptance for the $K^+ \to \pi^+ \nu\bar{\nu}$ decay. Every mirror in a half-mosaic must be properly oriented so that its centre of curvature coincides with the nominal one of the half-mosaic. Two different techniques are employed to measure the orientation of each mirror, whose angular position can be adjusted until the mirror is properly oriented:

- laser alignment (accuracy $\sim$ 500 μrad in terms of mirror orientation): during installation and after interventions inside the RICH vessel, a laser beam reflected by a specific point of the mirror is used to determine the mirror orientation;
- alignment with data (accuracy $\sim$ 30 μrad): during data taking, the orientation of each mirror is measured by comparing the flight direction of charged particles measured by the RICH to that measured by the Straw spectrometer.

2017 JINST 12 P12017

In this section the "laser alignment" procedure is described, while the "alignment with data" is beyond the scope of this paper. Mirrors need to be properly oriented at three different stages of installation:

1. just after placing the mirror on the corresponding dowel, its angular position is adjusted by means of two threaded aluminum pins pushing two points on the back of the mirror below its barycenter; once the mirror is properly oriented its stabilizing ribbons are precisely cut before connecting them to the piezo-electric motors;
2. after installing the stabilizing ribbons, the pins are removed and the mirror is oriented turning the adjusting screw on the joints connecting stabilizing ribbons to piezo-electric motors;
3. finally, after completing the installation of all mirrors, their orientation is checked again and finely tuned using piezo-electric motors.

7.1 Operation principles

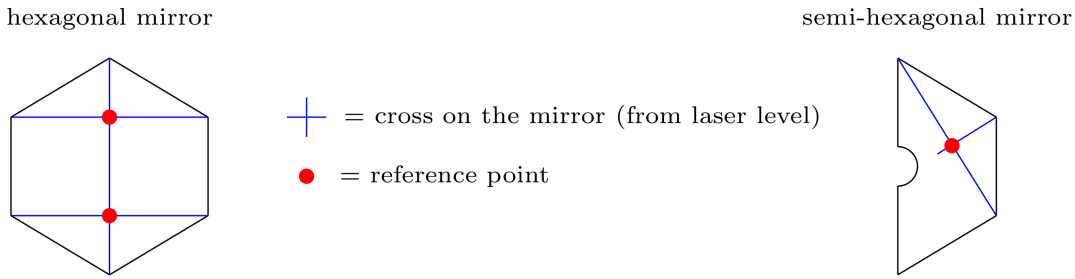

Figure 17. Reference points on hexagonal and semi-hexagonal mirrors.

The ideal way to determine the correct orientation of a spherical mirror would be to illuminate a point of the mirror with a light beam coming from the nominal centre of curvature and rotate the mirror until the light is reflected to the beam source. However the nominal centres of curvature of the two half-mosaics are located outside the vessel (17 m upstream of its upstream end) and are not visible from the mirror mosaic. It was therefore necessary to place the light source closer to the mirror mosaic.

A light beam impinging on a point P of a properly oriented mirror is reflected back to its source if and only if the light source is placed on the line joining the point P with the nominal centre of curvature. Thus, the correct positioning of the light source depends not only on the position of the nominal centre of curvature (the same for all mirrors in a half-mosaic) but also on that of the point P on the mirror. Two well-defined points of each mirror are chosen for this purpose. For each hexagonal mirror two reference points are defined ("upper reference point" and "lower reference point') lying on its vertical symmetry axis, i.e. the vertical line joining the uppermost and lowermost vertices of the hexagon. The two reference points are located at the same height as the hexagon lateral vertices, as shown in figure 17-left. A laser level projecting a cross (two orthogonal lines) on the mirror is used to precisely identify the chosen reference point. For semi-hexagonal mirrors the upper and lower reference points are defined as the intersection of a line connecting two non-adjacent vertices and the perpendicular to this line drawn from another vertex (see figure 17-right).

The position of each reference point in the NA62 reference frame is derived from that of the dowel supporting the mirror, precisely measured by CERN survey service, and the mirror geometry (relative positions of vertices and support blind hole) measured as described in section 3.1.

For practical reasons, the laser beam is sent to a mirror reference point from a direction close, but not coincident, to that coming from the nominal centre of curvature. The position of the reflected beam on a screen near the light source is compared to the expected one calculated assuming the mirror is properly oriented. From the position of the beam spot relative to the expected one, the rotation angles (θ_x, θ_y), needed to adjust the mirror orientation, are determined.

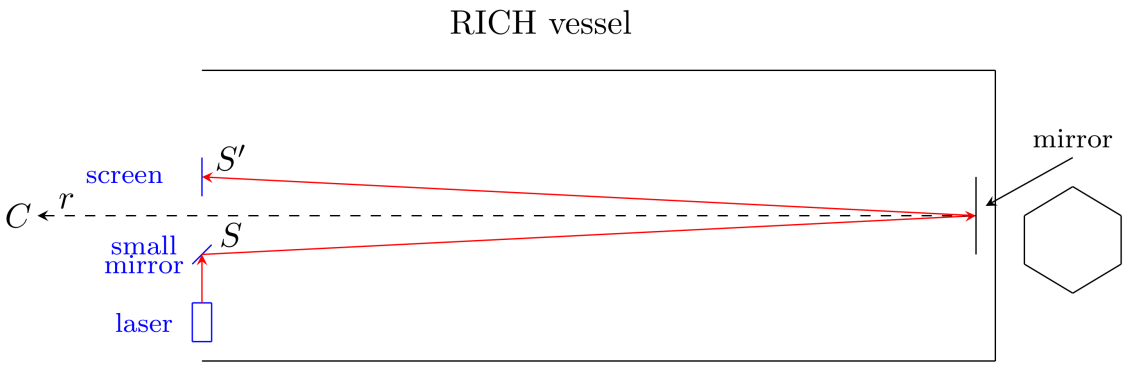

Figure 18. Scheme of the laser alignment system.

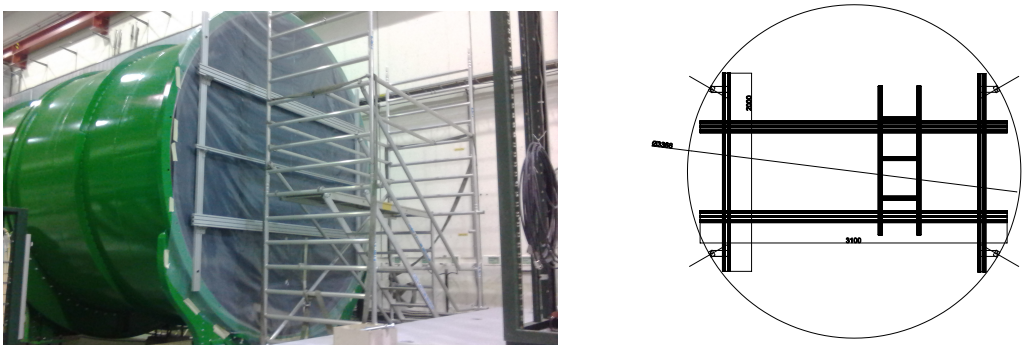

Figure 19. Left: the 2014 laser alignment support structure (at the upstream end of the RICH vessel). Right: the 2016 laser alignment support structure (inside the RICH vessel).

7.2 Laser alignment

The alignment system, sketched in figure 18, consists of a He-Ne laser source, a small orientable mirror mounted on a horizontal platform and a vertical screen equipped with millimeter paper. The platform and the screen can be positioned at different heights on a support structure ("ladder"), which can translate horizontally along rails placed perpendicularly to the axis of the RICH vessel. Figure 19-left shows the mechanical structure supporting the laser alignment equipment.

The positions of several reference points on the platform and the screen have been measured by CERN survey service. The platform and the screen can be moved to a different position by a

2017 JINST 12 P12017

rigid translation in the xy plane.[6] Measuring tapes fixed to the "ladder" and to one of the rails are used to determine the new positions. The central part of the small orientable mirror on the platform acts as a small-size light source placed at a well defined position, while the vertical screen allows to compare the position of the reflected beam to the one calculated assuming the mosaic mirror is properly oriented. The difference between these positions allows to determine how much the mirror has to be rotated about x and y axes to reach the correct orientation.

In 2014, during and after installation of the RICH mirror mosaic, the laser alignment system was positioned at the upstream end of the RICH vessel. This position, at large distance (17 m) from the mirror mosaic, provides a good sensitivity to mirror orientation (34 mm/mrad). The measured displacement roughly corresponds to that of the centre of the Cherenkov ring at the PMTs flange. The laser alignment system has been dismounted after mirror installation before installing the upstream closure of the RICH vessel.

In September 2014, during the installation of the beam pipe inside the RICH vessel, the pipe touched the central semihexagonal mirrors, producing large changes in the orientation of several mirrors. These mirrors (all but one of the semihexagonal central mirrors) have been re-oriented by "laser alignment" method performed by using a different setup. The orientation precision could not be as good as the previous one (the alignment equipment was placed on a tripod and its position was known with a larger uncertainty), but was largely sufficient to keep reflected Cherenkov light within the PMTs acceptance.

After the replacement of the semi-hexagonal mirrors during the technical stop of winter 2015-2016 the laser alignment was performed again. The upstream part of the RICH vessel was not accessible during these activities, the laser alignment apparatus has been positioned inside the vessel (see figure 19-right), 10 m away from the mirror mosaic, providing a sensitivity of 10 mm/mrad which corresponds to a 500 μrad accuracy in terms of the mirror orientation.

8 Conclusions

In this paper the details of the NA62 RICH mirror system are described. Geometry and optical parameters of each mirror were measured before the installation. The installation and alignment of the mirrors were performed and achieved the requested accuracy.

Acknowledgments

The construction of the RICH detector would have been impossible without the enthusiastic work of many technicians from University and INFN of Perugia and Firenze, the staff of the CERN laboratory and the strong collaboration with INFN Ferrara. We are grateful to the whole NA62 Collaboration for its support during the construction, installation and commissioning of the RICH detector and for its dedication in operating the experiment in data taking conditions.

References

[1] G. Anelli et al., *Proposal to measure the rare decay $K^+ \to \pi^+ \nu\bar{\nu}$ at the CERN SPS*, CERN-SPSC-2005-013 (2005) [CERN-SPSC-P-326].

[6] The small rotation due to the bending of horizontal rails can be neglected.

2017 JINST 12 P12017

[2] E. Cortina Gil et al., *The beam and detector of the NA62 experiment at CERN*, 2017 *JINST* **12** P05025.

[3] G. Anzivino et al., *Construction and test of a RICH prototype for the NA62 experiment*, *Nucl. Instrum. Meth. Phys.* **A 538** (2008) 314.

[4] B. Angelucci et al., *Pion-Muon separation with a RICH prototype for the NA62 experiment*, *Nucl. Instrum. Meth.* **A 621** (2010) 205.

2017 JINST 12 P12017